Anti-swing Control of Quadrotors during Human Interaction: An Adaptive Approach

Thesis submitted in partial fulfillment
of the requirements for the degree of

Master of Science in
Electronics and Communication Engineering
by Research

by

ANANTH RACHAKONDA
2021702025
ANANTH.RACHAKONDA@RESEARCH.IIIT.AC.IN

International Institute of Information Technology
Hyderabad - 500 032, INDIA
February 2024

International Institute of Information Technology
Hyderabad, India

CERTIFICATE

It is certified that the work contained in this thesis, titled "Anti-swing Control of Quadrotors during Human Interaction: An Adaptive Approach" by Ananth Rachakonda, has been carried out under my supervision and is not submitted elsewhere for a degree.

Date	Adviser: Prof. SPANDAN ROY

To My Parents and Teachers

Acknowledgments

Richard Feynmann's words "You can know the name of a bird in all the languages of the world, but when you're finished, you'll know absolutely nothing whatever about the bird... So let's look at the bird and see what it's doing — that's what counts." capture the ideals of my quest for understanding systems and I thank every person who's voluntarily or involuntarily been part of it. I dedicate this thesis to each of them.

First and foremost, I am grateful to Prof. Spandan Roy for believing and giving me an opportunity to explore and conduct research in advanced controls at the Robotics Research Center, IIIT Hyderabad. I am fortunate to have found a mentor for research in him. I am very grateful to Prof. Madhava Krishna for nurturing my ideas and pointing me to unexplored research territory. I am immensely grateful to my parents for their incredible support, trust and encouragement. I am thankful for the guidance I found in my senior research colleagues, Swati Dantu and Rishabh Dev Yadav.

I am thankful for the continuous inspiration from the members of my family and their non-academic guidance during my undergraduate degree. I am fortunate to have had teachers Mr. Emmanuel, Mr. Manivannan, Mrs. Sowmya, Mrs. Jyotsna, Mrs. Bindu Nair, lecturer Mr. Vinayaka Rao, music teachers Mr. Raman Kalyan, Mr. Hemanth, and academic mentors Prof. Spandan Roy and Prof. Madhav Krishna at important junctures of life, all who trusted in my capacity to discover, perform, persevere, and create for which I am immensely grateful. I am thankful to have remained in touch with Niharika Amajala for the deep talk, Kaustab Pal for being the older friend on campus, Sudarshan Harithas for academic banter, Omama, Rahul Sajnani, Girish Nandiraju, Amartya Sasi Kiran, Jhanvi Shigala and Swati Dantu for being the best of friends.

I am thankful to the Robotics Research Center (RRC), which welcomed me with open arms. I owe my progress to each non-academic staff of IIITH just as much, for their support allowed in the timely completion of my degree.

Finally, I thank the institute for providing a stimulating atmosphere, allowing dreams of budding researchers to blossom into impactful work.I also appreciate the thesis examiners for their valuable feedback, which helped me improve this thesis.

Abstract

In the field of aerial transport, specifically in operations involving quadrotors carrying suspended payloads, two critical stages are the attachment and detachment of the payload. These procedures are challenging due to various uncertainties inherent in the quadrotor, environmental variables, and payload swings caused by human or external interactions. These uncertainties can escalate quickly, posing significant risks to the quadrotor and payload and, crucially, to the human operator involved in the attachment/detachment process.

Current advanced controllers in this field often need to adequately address these uncertainties, typically treating them as bounded, predictable variables. However, this approach must be revised to manage the unpredictable nature of payload swings during these critical stages. To overcome this limitation, our research introduces an innovative adaptive anti-swing controller. This controller uniquely considers uncertainties state-dependently, specifically tailored to address swing induced by the unpredictable aspects of attaching and detaching suspended payloads.

In this work, we have conducted a thorough analytical evaluation of the closed-loop stability of this new system. Additionally, real-time experimental trials have been carried out. The results from these experiments demonstrate a marked performance improvement compared to existing state-of-the-art systems. This novel approach shows promise in enhancing safety and control effectiveness in aerial payload transportation, especially during the vital phases of payload and unclasping.

Contents

List of Figures

List of Tables

Chapter 1

Introduction

Robotics, a transformative reality, and a testament of human will to manifest fiction, has metamorphosed the life of both the common man and the industry. A progression from simple machinery to sentient agents is being driven by relentless innovation and technological advancements. In the enthralling realm of robotics, the elegance of machines is matched only by their steadfast commitment to safety. This is not merely a display of technological prowess but a critical ballet of intelligent machines that inherently safeguard their human and environmental counterparts.

Central to this journey is the development of advanced control systems, crucial for reliable and efficient robots. These systems not only reflect technical ingenuity but also underscore an important aspect of robotics: a tangible realisation of autonomy.

Humans have long sought ways to extend their capabilities and overcome physical limitations. Robotics presents a solution to this quest, offering the power to handle tasks that are either too dangerous, too precise, or too tedious for humans. This realization has been a driving force in the development of robotics, particularly in fields where the power and precision of robots significantly enhance efficiency and safety.

Then, robots by their very build, target capabilities that surpass human limitations. This capacity reaps from performative hardware and software design. Unlike humans, who are subject to fatigue, physical strain, and limitations in precision and strength, robots can be engineered to perform tasks with greater ease, accuracy, and endurance. Similarly, robots, through software considerations, can be built to perform repeatably, reliably, and safely over extended periods. Tasks such as lifting heavy objects, executing precise surgical procedures, or enduring hazardous conditions without degradation in performance, and safe payload transportation.

In robotic systems, the development of control technologies as part of their software design has played a crucial role. Autonomous vehicles and mobile robots, once figments of imagination, have become practical realities due to feedback control advancements. These vehicles are used widely, from research to commercial applications, and come in various forms like wheeled, marine, and aerial robots. Despite the limited use of aerial and marine robots due to safety concerns, road vehicles with autopilot features are becoming commonplace, leading major automobile manufacturers to pivot towards autonomous vehicle technology.

The control of these autonomous systems spans a wide spectrum. High-level control, for instance, involves selecting optimal trajectories, while low-level control focuses on specific actuator inputs. These control levels range from strategic path planning to the detailed calculation of forces and torques required for precise movement and task execution. This hierarchy of control underscores the robots' ability to perform complex tasks safely and efficiently, which are hazardous for humans.

Robotics is a convergence of human aspiration, technological advancement, and an inherent commitment to safety and efficiency. Developmental advances in Safety Critical Controls ensure that the effort is directed towards enhancing human capabilities while safeguarding human interests.

1.1 Aerial Robotics

Aerial robots exemplify humanity's quest to transcend physical boundaries, utilizing aerial transportation to leverage the third dimension for more efficient travel. This advancement addresses a fundamental challenge in modern transportation, as many autonomous vehicle researchers note: adding an aerial dimension could be a solution to the rapidly increasing problems of road traffic congestion.

Aerial vehicles are primarily categorized into two types based on their design: fixed-wing aircraft and rotary-wing quadrotors. The emergence of Unmanned Aerial Vehicles (UAVs) marks a significant milestone in aerial vehicle applications. UAVs can be either autonomous or remotely operated, but in both scenarios, control is a critical aspect. This research particularly focuses on the low-level control of quadrotors, a vital area due to the absence of a braking mechanism in aerial robots, which makes stability control more crucial than in ground-based robots, like rovers.

Fixed-wing aircraft, with their mechanically advantageous design, are well-suited for transporting cargo and passengers. They are extensively used for various purposes, including personal, commercial, research, and defense activities. However, fixed-wing aircraft have limitations: they require runways for takeoff, have a non-holonomic design, and cannot hover in place. These constraints render them impractical for certain applications like indoor goods transfer, disaster relief, and surveying, paving the way for the utility of rotary-wing quadrotors in these scenarios.

1.2 System Dynamics

The main components involved in modeling a robotic system, namely, representing the model, defining reference frames with state variables, and developing kinematic and dynamic dynamic equations. Although there are various approaches to modeling dynamics in each of these sections, the focus will be on the method employed in this work.

1.2.1 Reference Frames

Identifying reference frames is a key aspect in the dynamic modeling process, particularly for quadrotor applications. Two types of frames are commonly used to simplify the representation: an inertial frame, which describes the quadrotor's absolute position and orientation, and a body-fixed frame, which is used to depict the forces and torques acting on the quadrotor's body.

Inertial Frame

The inertial reference frame is defined as a frame in which a body, not influenced by any net force, remains at rest or moves in a straight line. It's commonly associated with a ground-fixed plane, and if we disregard Earth's movement, this frame can be considered stationary. Often referred to as the World frame, it is oriented with the X-axis pointing forward, the Z-axis pointing upwards, and the Y-axis determined by the right-hand rule. The differential equations used to depict the system's dynamics are formulated with respect to this inertial frame reference.

Body-Fixed Frame

The body-fixed frame is attached directly to the quadrotor and adheres to the same axes convention as the inertial frame. Each frame consists of three orthonormal axes that intersect at the center-of-mass (CoM). For simplicity, these axes are selected to be the principal axes in the body-fixed frame, mirroring those in the inertial frame. The forces exerted by the propellers impact this body-fixed frame. In the case of a quadrotor, the thrust generated by the motors

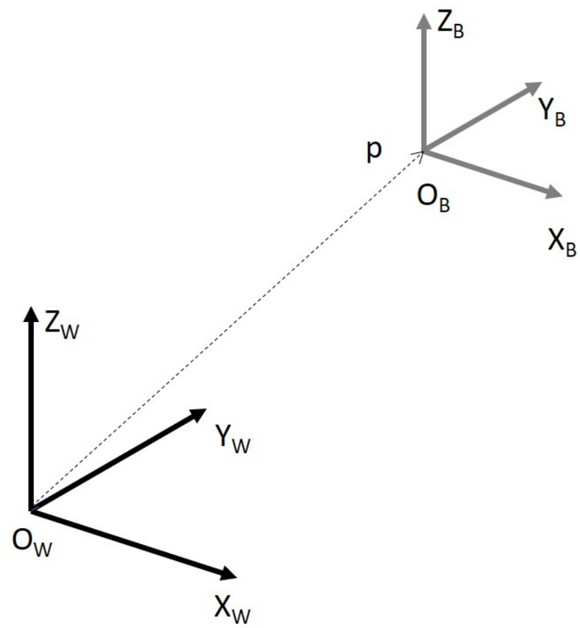

Figure 1.1: A schematic of reference frames.

results in forces and torques within this frame. Therefore, the quadrotor's angular velocities are described in terms of the body-fixed frame.

In Figure 1.1, the inertial and body-fixed frames are depicted, having their origins at O_W and O_B, respectively. The position vector p represents the relative position of the quadrotor's center-of-mass (which is also the origin of the body-fixed frame) in relation to the inertial frame.

1.2.2 Quadrotor Dynamics

The final aspect of modeling involves formulating the dynamic equations for the system.

In a quadrotor, the forces and torques are generated solely by the propellers' rotation. Each propeller exerts an upward force along the Z_B axis of the body-frame, and produces two distinct types of torques: one resulting from the upward force along the X_B and Y_B axes, and the other arising from the propellers' rotation, creating a torque around the Z_B axis. To simplify the dynamics, the quadrotor is symmetrically designed around the origin in the X_BY_B plane. Additionally, the Center of Mass (CoM), denoted as O_B, is aligned with the propeller plane.

The body frame of the quadrotor is structured such that its origin is at the CoM, with the X_B and Y_B axes aligned along two opposite arms (the rods connecting the center to the rotors), positioned at 45 degrees to either side of an arm. This design comes in two configurations: the

Figure 1.2: A picture of Q450 quadrotor with “x” configuration.

”+” (plus) configuration and the ”x” configuration (as shown in Fig. 1.2). In this discussion, we focus on the dynamics of the quadrotor in the ”x” configuration.

When all propellers rotate at the same speed and in the same direction, the torques along the X_B and Y_B axes are neutralized by the opposing propellers. However, the combined torque around the Z_B-axis increases, causing the quadrotor to rotate around this axis while maintaining its position. To balance this, opposite propellers spin in opposite directions, while adjacent ones rotate in the same direction.

Since the rotors point downwards, the thrust of the quadrotor is directed along the negative Z_B-axis. This thrust propels the quadrotor upward, countering gravity, especially when the Z_B-axis of the body frame aligns with the Z_W-axis of the world frame. Movements along the X_B and Y_B axes are generated by tilting or rolling the quadrotor. For instance, to pitch forward, the front motors slow down compared to the rear ones. To roll to the right, the left motors spin faster than those on the right, and the reverse is true for a left roll. Differences in rotor speeds can create uneven torques, causing the quadrotor to yaw. To prevent this, the total speeds of opposite motors are kept equal.

In this study, we adopt a dynamic model for the quadrotor that is widely recognized in several key works, such as those cited in [1], [2], and [3]. This model establishes the connection between the thrust T_{th}, the torques $\tau_\phi, \tau_\theta, \tau_\psi$, and the rotor speeds ω_i, for $i = 1, 2, 3, 4$.

$$\begin{bmatrix} T_{th} \\ \tau_\phi \\ \tau_\theta \\ \tau_\psi \end{bmatrix} = \begin{bmatrix} C_T & C_T & C_T & C_T \\ 0 & lC_T & 0 & -lC_T \\ -lC_T & 0 & lC_T & 0 \\ -C_TC_M & C_TC_M & -C_TC_M & C_TC_M \end{bmatrix} \begin{bmatrix} \omega_1^2 \\ \omega_2^2 \\ \omega_3^2 \\ \omega_4^2 \end{bmatrix} \tag{1.1}$$

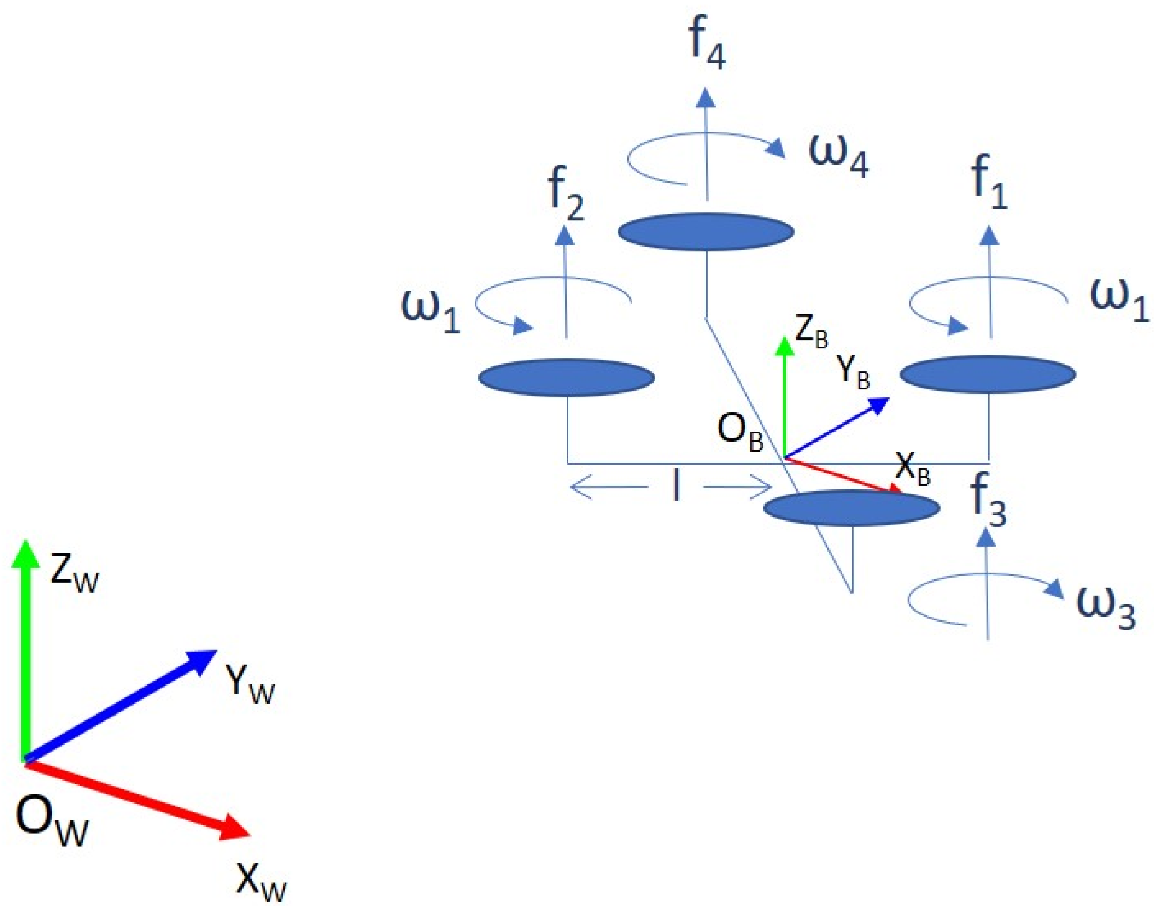

Figure 1.3: A schematic representing a quadrotor's dynamics.

where C_T and C_M are thrust constant and moment constant respectively, and l is the arm-length (please refer to Fig 1.3).

In the absence of external disturbances, the quadrotor encounters only a limited set of forces and torques besides gravity. According to the equations, the control variables are the rotors' angular velocities. Managing these velocities allows control over the upward thrust, as well as the roll, pitch, and yaw of the quadrotor. Control of movement in other directions is achieved indirectly through the manipulation of roll and pitch. Therefore, the quadrotor is an underactuated system, with four control inputs governing its six Degrees of Freedom (DoF).

The primary linear forces influencing the system are the gravitational force, G, directed along the negative Z_W-axis in the inertial frame, and the thrust, T_{th}, exerted along the positive Z_B-axis in the body frame. Consequently, the linear dynamics of the system are represented as shown in reference 1.2.

$$m \begin{bmatrix} \ddot{x} \\ \ddot{y} \\ \ddot{z} \end{bmatrix} + \begin{bmatrix} 0 \\ 0 \\ mg \end{bmatrix} = \mathbf{R}^T \begin{bmatrix} 0 \\ 0 \\ T_{th} \end{bmatrix} \tag{1.2}$$

where g represents the acceleration caused by gravity, m is the quadrotor's total mass, and R is the rotational matrix employed to convert forces from the inertial frame to the body-fixed frame. Due to the characteristics of orthonormal matrices, the transpose of R, denoted as R^T, is used to transform vectors from the body frame back to the inertial frame. The rotational dynamics of the system are described in the following manner.

$$\begin{aligned} &\frac{I_{xx}}{l}\ddot{\phi} + \frac{I_{zz} - I_{yy}}{l}\dot{\varphi}\dot{\psi} = \tau_\phi, \\ &\frac{I_{yy}}{l}\ddot{\varphi} + \frac{I_{xx} - I_{zz}}{l}\dot{\phi}\dot{\psi} = \tau_\varphi, \\ &I_{zz}\ddot{\psi} + (I_{yy} - I_{xx})\dot{\varphi}\dot{\phi} = \tau_\psi, \end{aligned} \tag{1.3}$$

where l is arm-length of the rotor units; I_{xx}, I_{yy}, I_{zz} are the inertia terms in x, y and z directions respectively. The rotation matrix R is given by

$$\mathbf{R} = \begin{bmatrix} c_\psi c_\varphi & s_\psi c_\varphi & -s_\varphi \\ c_\psi s_\varphi s_\phi - s_\psi c_\phi & s_\psi s_\varphi s_\phi + c_\psi c_\phi & s_\phi c_\varphi \\ c_\psi s_\varphi c_\phi + s_\psi s_\phi & s_\psi s_\varphi c_\phi - c_\psi s_\phi & c_\varphi c_\phi \end{bmatrix}$$

where, $c_{(\cdot)}, s_{(\cdot)}$ denote $\cos_{(\cdot)}, \sin_{(\cdot)}$; m is the mass of the overall system.

In this work, we have used the following quadrotor dynamics.

$$\begin{aligned} \mathbf{M_p}\ddot{\mathbf{p}} + \mathbf{G} &= \mathcal{T}_\mathbf{p} \\ \mathbf{M_q}(\mathbf{q})\ddot{\mathbf{q}} + \mathbf{C_q}(\dot{\mathbf{q}})\dot{\mathbf{q}} &= \mathcal{T}_\mathbf{q} \end{aligned} \tag{1.4}$$

with

$$\mathbf{M_p} = \begin{bmatrix} m & 0 & 0 \\ 0 & m & 0 \\ 0 & 0 & m \end{bmatrix}, \ \mathbf{M_q} = \begin{bmatrix} \frac{I_{xx}}{l} & 0 & 0 \\ 0 & \frac{I_{yy}}{l} & 0 \\ 0 & 0 & I_{zz} \end{bmatrix}, \ \mathbf{G} = \begin{bmatrix} 0 \\ 0 \\ mg \end{bmatrix}$$
$$\mathbf{C_q} = \begin{bmatrix} 0 & 0 & \frac{I_{zz}-I_{yy}}{l}\dot{\varphi} \\ \frac{I_{xx}-Izz}{l}\dot{\psi} & 0 & 0 \\ 0 & \frac{I_{yy}-Ixx}{l}\dot{\phi} & 0 \end{bmatrix}, \ \mathbf{p} = \begin{bmatrix} x \\ y \\ z \end{bmatrix}, \ \mathbf{q} = \begin{bmatrix} \phi \\ \varphi \\ \psi \end{bmatrix}$$
$$\mathcal{T}_\mathbf{p} = \begin{bmatrix} \tau_x \\ \tau_y \\ \tau_z \end{bmatrix}, \ \mathcal{T}_\mathbf{q} = \begin{bmatrix} \tau_\phi \\ \tau_\varphi \\ \tau_\psi \end{bmatrix} \tag{1.5}$$

where, $\mathbf{M_p}$ and $\mathbf{M_q}$ are diagonal matrices that represent the mass and inertia of the quadrotor respectively; $\mathbf{C_q}$ is the Coriolis matrix containing the cross-coupling terms; $\mathbf{p}$ and $\mathbf{q}$ are the position and orientation vectors of the quadrotor in the inertial frame, $\mathbf{G}$ is the gravity vector and $\mathcal{T}_\mathbf{p}$ and $\mathcal{T}_\mathbf{q}$ are the force and moment vectors acting on the CoM of the quadrotor.

1.3 Control of Quadrotors

The initial works of quadrotor control were focused on reducing the complexity of the dynamics of the quadrotor. The simplest of all is the hovering mode control, where the quadrotor is assumed to have no disturbances across the X_W and Y_W axes. This type of control can be used to hover the quadrotor at any given height, and thus, only controlling the altitude of the quadrotor was sufficient. The earliest of control designs was well-proven Proportional-Integral-Derivative (PID) controller [4–6].

The evolution of quadrotor control progressed beyond the limited scope of hovering mode, leading to the development of feedback linearization, also referenced in works like [7–9]. This method is often termed as small-angle variation control, owing to its assumption that variations in roll and pitch angles are relatively minor. It's particularly suited for flying modes close to hovering, and adaptive controllers designed for these conditions are discussed in [10]. While control based on small-angle approximations is straightforward to implement, it may become unstable during more dynamic or aggressive flight maneuvers of the quadrotors.

A key advancement in quadrotor control is the introduction of the geometric controller, as detailed in [1]. This research presented a partially decoupled dynamic model for the quadrotor (refer to Chapter 2 for more details) along with a dual-loop control system. The application of geometric control within the rotation matrices' manifold makes it highly effective for executing complex maneuvers. Another significant contribution in this field was made by [11] and their team, who developed a fully decoupled dynamic model for quadrotors. However, this model remains largely theoretical and requires additional mechanical structures for practical implementation, such as the tiltrotor mechanism discussed in [12, 13]. For a comprehensive overview of current control strategies for autonomous quadrotors, the survey in [14] is an excellent resource.

However, the research mentioned above, including the references within, relies significantly on precise system modeling and dynamics. In practical scenarios, accurately modeling a quadrotor's exact dynamics is challenging and often unfeasible due to factors like non-linearities, imprecise parameter knowledge, uneven mass distribution, and external disturbances. Additionally, when quadrotors are utilized in applications like surveying, manipulation, or transporting payloads, as mentioned in [15–17], their dynamics can vary due to changes in the payload. In this thesis, we specifically explore two types of aerial transportation, addressing the control challenges and solutions associated with each. These two scenarios are discussed in the following sections:

1.3.1 Adaptive Control of Quadrotors with Cable-suspended Payload

In recent times, there's been considerable interest in using quadrotors or similar aerial vehicles for delivering payloads in various civilian and military contexts, as discussed in studies like [18–20]. When it comes to aerial payload transport, the two predominant methods are cable-suspended (refer to [16, 21–23]) and gripper-attached (see [11, 24–26]). The cable-suspended approach is often favored for its ability to handle different payload sizes while maintaining the quadrotor's nimbleness. This method, however, introduces a greater control challenge due to the additional unactuated degrees-of-freedom from the payload's swing angles, adding to the already underactuated nature of the quadrotor.

Key operations in cable-suspended transportation include attaching and detaching payloads, often requiring human interaction (as shown in Fig. 1.4). For the safety of those involved, it's crucial that the quadrotor can stabilize itself against the disturbances caused by the payload's swing.

Regrettably, as noted in the literature, controlling such a system in the presence of uncertainties (like parametric changes, wind, and rotor downwash) is difficult. The payload's swing angles add more unactuated degrees-of-freedom to the quadrotor, making the control of this underactuated system a complex challenge.

1.3.2 Beyond Payload Clasp and Unclasp: Inflight Interaction with Cable-suspended Payload

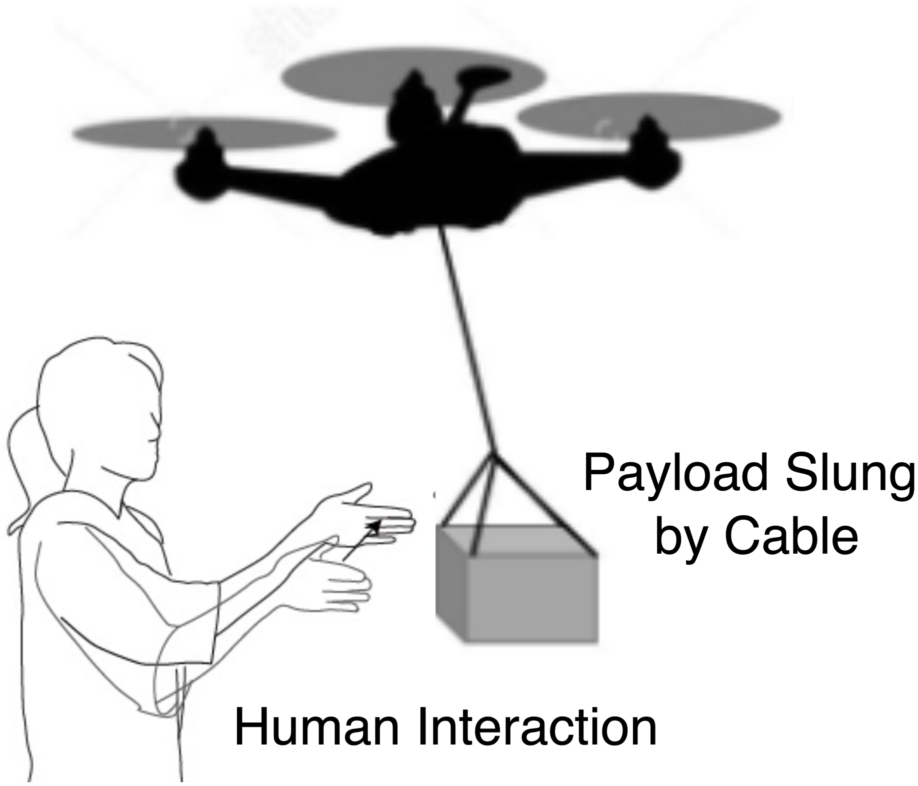

Figure 1.4: A diagram representing a human interacting with the suspended payload carried by a quadrotor

In the previous scenario, it is only assumed that the payload will be clasped and unclasped during the flight. However, in a typical assignment or emergency evacuation, a quadrotor might be mounted with a cable-suspended payload during hover which may also induce aggressive swing, if the payload and the quadcopter are at different heights such that the cable holding the payload is not taut initially, especially in the case where the payload is being picked from high rises. This will induce unwanted payload swing. Dynamic variations in suspended payload are orchestrated by these situations. One such orchestration is illustrated by deliberately changing both the payload swing angle and the height aggressively with a stick. Fig. 1.5 in 4 phases: (i) in the first phase, the quadrotor hovers in the air with the suspended payload (ii) in the second phase, the suspended payload is perturbed with a stick; (iii) and in the third phase, the suspended payload is observed to be displaced far from its initial configuration (iv) In the fourth phase the quadrotor is trying to stabilize the suspended payload. Similar phases can be observed during a construction scenario.

1.3.3 Human-Payload Interaction: In-flight Payload Perturbation

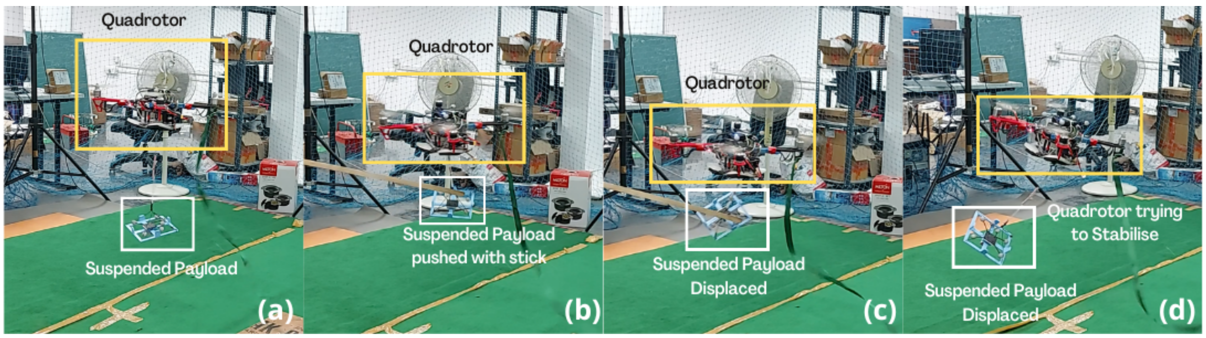

Figure 1.5: A 4 stage representation of induced sing in cable suspended payload due to pickup scenario, human interaction, or accidental clasp/unclasp

Though robust controllers [27–31] might solve the problem of variation in dynamics to an extent, they also suffer when bounds of uncertainties are unknown. Hence, an adaptive controller is typically employed to solve these issues [17, 25, 32–39]. However, adaptive control typically requires structural knowledge of the system and cannot handle unmodelled dynamics, and such prerequisites are difficult to meet in the cases of unknown payload transport. Further, it is well-known that under a changing dynamics, typically arising during dynamic payload swing, conventional controllers are not suitable [40–45]. In addition, to the best of our knowledge, no control solution exists to efficiently dampen the payload swing of a quadrotor in an adaptive setting. This thesis aims to solve these control challenges.

1.4 Preliminaries

1.4.1 Stability Notions

An autonomous nonlinear system represented by the following dynamic equation

$$\dot{x} = f(x(t)), \quad x(0) = x_0$$

where $x(t) \in \mathbb{R}^n$ represents the system state vector is said to be stable, the function f attains an equilibrium at the point $x = x_e$, i.e, $f(x_e) = 0$ and $f'(x_e) = 0$.

The equilibrium point is said to be:

- **Stable**, if there exists a bound $\epsilon > 0, \delta > 0$ such that $|x(0) - x_e| < \delta \implies |x(t) - x_e| < \epsilon, \quad \forall t \geq 0$. Stability makes sure the states starting from close enough to a bound δ will remain within the bound ϵ.

- **Asymptotically stable**, if in addition to being stable, $\lim_{t \to \infty} \|x(t) - x_e\| = 0$. Therefore, the system not only remains within the bound ϵ but also converges to the equilibrium point.

- **Exponentially stable**, if in addition with asymptotic stability there exists $\alpha > 0, \beta > 0, \delta > 0$ such that $\|x(t) - x_e\| \leq \alpha \|x(0) - x_e\| e^{-\beta t}, \quad \forall t \geq 0$. Hence, system converges to the equilibrium at an exponential rate.

- **Uniformly Ultimately Bound (UUB):** The solutions of $\dot{x} = f(x(t))$ is said to be uniformly ultimately bound with ultimate bound b if $\exists b > 0$, $c > 0$ and for every $0 < a < c$, $\exists T = T(a, b) > 0$ such that

$$||x(t_0)|| \leq a \implies ||x(t)|| \leq b, \quad \forall t \geq t_o + T. \tag{1.6}$$

1.5 Contributions of the Thesis

In this thesis, advancements have been made in the field of adaptive control systems for quadrotors with suspended payloads, specifically targeting safe human-quadrotor interactions. The key contributions of this research are summarized as follows:

1. **Development of an Adaptive Anti-Swing Controller:** This research introduces an innovative adaptive anti-swing controller tailored for human-quadrotor interaction. The controller is uniquely designed to manage the state-dependent uncertainties inherent in the dynamics of suspended payloads. This is a critical advancement over existing methods, as it effectively handles unknown dynamic variations without prior knowledge of specific uncertainty terms.

2. **Formulation and Analysis of a Controller for Enhanced Safety and Precision in Human-Quadrotor Interacting Systems:** The proposed control framework significantly improves the safety and precision of human-quadrotor interactions, especially during critical operations like clasping and unclasping of cable-suspended payloads. The safety aspect is a pivotal focus of this research, addressing a key challenge in the field.

3. **Experimental Validation of Performance surpassing State-of-the-Art Methods:** Comparative experimental investigations have demonstrated that the adaptive control approach developed in this thesis outperforms existing state-of-the-art methods. The controller exhibits a remarkable ability to mitigate undesired payload swings, which is a testament to its efficacy.

4. **Discussion on the Impact on Future Human-Interacting Quadrotor Applications:** The findings and developments from this thesis have significant implications for future applications in the field of quadrotor technology, especially in scenarios requiring direct human interaction. The adaptive anti-swing control approach sets a new benchmark for operational safety and control precision in such contexts.

These contributions represent a valuable addition to the field of adaptive control for quadrotors, particularly in the context of human-quadrotor interaction carrying suspended payloads. The outcomes of this research not only address existing challenges but also pave the way for future innovations in aerial robotics.

1.6 Organization of the Thesis

The thesis is organized into four chapters. A brief summary of each chapter is mentioned below.

- **Chapter 1:** This introductory chapter gives an overview of quadrotors, their dynamic model and control strategies. It briefly describes the motivation for this research, the problem orientation, the pertaining gaps in the literature, the main contributions and an outline of the thesis.

- **Chapter 2:** This chapter explains a new adaptive anti-swing controller for quadrotors carrying suspended payloads that can handle payload swing and dampen it. The stability of the closed-loop system using the proposed controllers is studied using Lyapunov theory.

- **Chapter 3:** In this chapter the proposed controller's effectiveness is demonstrated through hardware experiments, showing how it outperformed state-of-the-art controller in terms of stability, convergence, and robustness to payload swing induced by human interaction. The performance is compared via error plots and root mean-squared (RMS) error.

- **Chapter 4:** This chapter concludes the thesis by summarizing the various contributions brought out by this thesis.

1.7 Symbols and Notations:

The symbols and notations used in the following chapters are as shown in Table 1.1

$\mathbb{R}$	Real line
$\mathbb{R}^+$	Real line of positive numbers
$\mathbb{R}^n$	Real space of dimension n
$\mathbb{R}^n$	Real matrix of dimension $n \times n$
$\exists$	there exists
$\forall$	for all
$\mathbf{I}$	Identity matrix
$\Xi > 0 (< 0)$	Positive (negative) definite matrix
$\lambda_{\min}(\Xi)$	Minimum eigen value of the matrix Ξ
$\lambda_{\max}(\Xi)$	Maximum eigen value of the matrix Ξ
$\|\|\Xi\|\|$	Euclidean norm of the matrix Ξ
$\mathrm{sgn}(x)$	Signum of x = $x/\|\|x\|\|$
$\mathrm{sat}(x, \varpi)$	Saturation of x = $\begin{cases} x/\|\|x\|\|, \ if \ \|\|x\|\| \geq \varpi \\ x/\varpi, \ otherwise \end{cases}$

Table 1.1: Nomenclature of various symbols and notations used in the thesis.

Chapter 2

Anti-swing Control of Quadrotors during Human Interaction: An Adaptive Approach

2.1 Introduction

In recent times, the utilization of quadrotor and similar aerial vehicles for payload delivery has garnered extensive attention in both civilian and military applications. This is evident from various studies and proposals [18–20]. Among the prevalent methods of payload transport by these vehicles, namely, cable-suspension [16, 21–23] and fixed gripper attachment [11, 24–26], the former is often preferred. Its advantage lies in its flexibility, allowing the transportation of variously sized payloads without compromising quadrotor agility. However, this method introduces the challenge of stabilizing the additional unactuated degrees-of-freedom due to payload swing, which adds complexity to the already underactuated quadrotor system.

A critical phase in the cable-suspension method involves the payload's clasping and unclasping, often requiring human interaction (as shown in Fig. 1.4). During these operations, the quadrotor must be capable of stabilizing itself against disturbances, such as those caused by payload swings, to ensure human safety.

Controlling a quadrotor in the presence of such uncertainties, including parametric variations, external forces like wind or rotor downwash, etc., is acknowledged as a complex challenge in current literature. Many studies have simplified this by considering only a single planar swing angle [46–49]. However, for realistic payload transportation scenarios, accounting for both planar swing angles is necessary (refer to Fig. 2.1). While adaptive controllers have been proposed for dual swing angles [22, 50–52], they often fall short in addressing state-dependent dynamics unique to quadrotors. These unmodelled forces, such as low-velocity drag, rotor downwash, or payload-induced coupling forces (discussed later in Remark 2), can lead to unwanted quadrotor movements. These movements, if unchecked, pose risks not only to the quadrotor and payload but also to the human involved in payload handling, as evidenced by experimental results in Sect. IV.

Given these challenges, the thesis argues for a control design that effectively stabilizes payload swing angles in the face of such state-dependent uncertainties. This work addresses a gap in existing research by presenting a novel solution. The key highlights of this work include:

- An adaptive anti-swing control mechanism that estimates unknown state-dependent dynamics and external disturbances without prior knowledge of these factors.
- A comprehensive closed-loop stability analysis employing the Lyapunov approach.
- Real-time experimental validations that demonstrate significant improvements in system stabilization, particularly against disturbances induced by payload swing, compared to existing methods.

This research builds upon and extends prior studies by some of the authors [53–55], by incorporating unactuated cable-suspended payload dynamics and avoiding acceleration feedback required in earlier models.

The rest of this chapter is organised as follows: section 2.2 gives the suspended payload dynamics of the quadrotor while mentioning the assumptions and the properties needed for the controller formulation. section 2.3 delves into the details of the controller design. Section 2.4 gives the stability analysis of the proposed controller.

2.2 System Dynamics and Problem Formulation

For the quadrotor system with suspended payload as in Fig. 2.1, the associated symbols and system parameters are defined in Table 2.1. For system modelling, we take the following standard assumption:

Assumption 1 *([17, 50, 51, 56])The cable connecting the payload and the quadrotor is attached to the center of mass of the quadrotor and it is massless, inelastic and always taut.*

Under the above assumption and employing the Euler-Lagrangian formulation (cf. [57,58]), the dynamic model of the composite system can be obtained as

$$M(q)\ddot{q} + C(q, \dot{q})\dot{q} + G(q) + d = [\tau_p^T \; \tau_q^T \; 0 \; 0]^T, \tag{2.1a}$$

$$\tau_p = R_B^W U, \tag{2.1b}$$

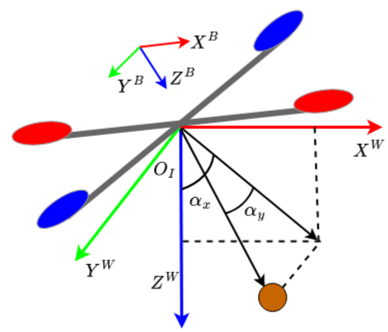

Figure 2.1: Illustration of a quadrotor system with suspended payload.

Table 2.1: Nomenclature

$[X^B\ Y^B\ Z^B]$	Quadrotor body-fixed coordinate frame
$[X^W\ Y^W\ Z^W]$	Earth-fixed coordinate frame
$[x\ y\ z]$	Quadrotor position in Earth-fixed coordinate frame
$[\phi\ \theta\ \psi]$	Quadrotor roll, pitch and yaw angles
α_x	Payload projection angles in $X^W Z^W$ plane
α_y	Payload projection angle in $Y^W Z^W$ plane
$M, C \in \mathbb{R}^{8\times 8}$	Mass and Coriolis matrices
$G \in \mathbb{R}^8$	Gravity vector
$d \in \mathbb{R}^8$	Unknown (state-dependent) dynamics vectors
$\tau_p, \tau_q \in \mathbb{R}^3$	Generalized control inputs

where $q(t) \triangleq \left[x(t), y(t), z(t), \phi(t), \theta(t), \psi(t), \alpha_x(t), \alpha_y(t)\right]$; $\tau_q(t) \triangleq [u_2(t),\ u_3(t),\ u_4(t)]$ is the control inputs for roll, pitch and yaw of the quadrotor; $\tau_p = R_B^W U$ is the generalized control input for quadrotor position in Earth-fixed frame, such that $U(t) \triangleq \begin{bmatrix} 0 & 0 & u_1(t) \end{bmatrix}^T$ being the force vector in body-fixed frame and R_B^W being the $Z - Y - X$ Euler angle rotation matrix describing the rotation from the body-fixed coordinate frame to the Earth-fixed frame [11]

$$R_B^W = \begin{bmatrix} c_\psi c_\theta & c_\psi s_\theta s_\phi - s_\psi c_\phi & c_\psi s_\theta c_\phi + s_\psi s_\phi \\ s_\psi c_\theta & s_\psi s_\theta s_\phi + c_\psi c_\phi & s_\psi s_\theta c_\phi - c_\psi s_\phi \\ -s_\eta & s_\phi c_\theta & c_\theta c_\phi \end{bmatrix}, \tag{2.2}$$

where $c_{(\cdot)}, s_{(\cdot)}$ are abbreviations for $\cos(\cdot), \sin(\cdot)$ respectively. The term $d(\dot{q}, t)$ represents combined effects of external disturbances (e.g., wind, gust) and unmodelled state-dependent dynamics (e.g., low speed aerodynamic drag forces, rotor downwash, ground reaction disturbance). Following the standard properties of Euler-Lagrange systems (cf. [59, Ch. 6]) and of aerial vehicles (cf. [50, 51], [60, Ch. 3]), we state the following standard system properties:

Property 1: $\exists \bar{c}, \bar{g}, \bar{d}_0, \bar{d}_1 \in \mathbb{R}^+$ such that $||C(q, \dot{q})|| \leq \bar{c}||\dot{q}||$, $||G(q)|| \leq \bar{g}$ and $||d(\dot{q}, t)|| \leq \bar{d}_0 + \bar{d}_1||\dot{q}||$.

Property 2: $M(q)$ is symmetric and uniformly positive definite. This implies that $\exists \mu_1, \mu_2 \in \mathbb{R}^+$ such that

$$0 < \mu_1 I_n \leq M(q) \leq \mu_2 I_n. \tag{2.3}$$

Consider the decomposition of M as $M = \hat{M} + \Delta M$, where $\hat{M}$ and ΔM represent the nominal and perturbation terms of the mass matrix, respectively. The amount of uncertainty in the system is framed as an assumption below, which acts as a control challenge:

Assumption 2 (Uncertainty) *Only the knowledge of $\hat{M}$ and an upper bound for ΔM is available, while the terms $C, G,$ d and their upper bounds $\bar{c}, \bar{g}, \bar{d}_0$ and $\bar{d}_1$ are unknown.*

Remark 1 (Importance of state-dependent uncertainty) *Property 1 highlights that the terms C and d create forces which directly depends on velocity; furthermore, motion in swing angles will excite motion in quadrotor via the coupling terms in inertia matrix M (cf. the structure in [57, 58]). Hence, uncertainty in these dynamic terms create state (i.e., velocity, acceleration)-dependent uncertainty. Crucially, it implies that these uncertainties, when unaddressed, will create unwanted motion in the system (cf. the system oscillations, drift etc. during the experiments later) leading to potential hazard.*

For controller design, as well as for convenience of notation, let us rewrite system (2.1a) as

$$M(q)\ddot{q} + N(q, \dot{q})\dot{q} + d = \begin{bmatrix} \tau^T & 0 & 0 \end{bmatrix}^T \tag{2.4}$$

where

$$\begin{aligned}
&q \triangleq [q_a,\ q_u],\ q_a = [x,\ y,\ z,\ \phi,\ \theta,\ \psi],\ q_u = [\alpha_x,\ \alpha_y] \\
&M \triangleq \begin{bmatrix} M_{aa} & M_{au} \\ M_{au}^T & M_{uu} \end{bmatrix}, \quad \begin{matrix} M_{aa} \in \mathbb{R}^{6\times 6}, M_{au} \in \mathbb{R}^{6\times 2} \\ M_{uu} \in \mathbb{R}^{2\times 2} \end{matrix}, \\
&N \triangleq C\dot{q} + G = [N_a,\ N_u],\ N_a \in \mathbb{R}^6, N_u \in \mathbb{R}^2, \\
&d \triangleq [d_a,\ d_u],\ d_a \in \mathbb{R}^6, d_u \in \mathbb{R}^2, \tau \triangleq [\tau_p,\ \tau_q].
\end{aligned}$$

Using these decomposed representations of M, N and d, the system dynamics (2.4) can further be represented as

$$\ddot{q}_u = -M_{uu}^{-1} M_{au}^T \ddot{q}_a + h_u, \tag{2.5a}$$
$$\ddot{q}_a = M_s^{-1} \tau + h_a, \tag{2.5b}$$

$$\begin{aligned} \text{where } h_u &\triangleq M_{uu}^{-1}(N_u + d_u), \\ h_a &\triangleq M_s^{-1}(N_a + d_a - M_{au} M_{uu}^{-1}(N_u + d_u)), \\ M_s &\triangleq M_{aa} - M_{au} M_{uu}^{-1} M_{au}^T. \end{aligned}$$

Control Objective: Under Assumptions 1-2 and Properties 1-2, to design an adaptive controller to maintain the quadrotor at a desired fixed location (x^d, y^d, z^d), while stabilizing the attitude and payload swing angles (i.e., $\phi^d = \theta^d = \psi^d = \alpha_x^d = \alpha_y^d = 0$).

The following section solves this control problem along with detailed analysis.

2.3 Proposed Controller Design

Let us define tracking error $e_a \triangleq q_a - q_a^d$ (q_a^d is a constant vector $[x^d, y^d, z^d, 0, 0, 0]$) and an auxiliary error variable r as

$$r \triangleq \Upsilon_a \dot{e}_a + \Gamma_a e_a + \Upsilon_u \dot{q}_u + \Gamma_u q_u, \tag{2.6}$$

where $\Upsilon_a, \Gamma_a \in \mathbb{R}^{6\times 6}$ are positive definite and $\Upsilon_u, \Gamma_u \in \mathbb{R}^{6\times 2}$ are full rank user-defined matrices.

Using (2.5a) and (2.5b), the time derivative of (2.6) yields

$$\begin{aligned} \dot{r} &= \Upsilon_a \ddot{q}_a + \Gamma_a \dot{e}_a + \Upsilon_u \ddot{q}_u + \Gamma_u \dot{q}_u \\ &= (\Upsilon_a - \Upsilon_u M_{uu}^{-1} M_{au}^T)(M_s^{-1}\tau + h_a) + \Upsilon_u h_u \\ &\qquad + \Gamma_a \dot{e}_a + \Gamma_u \dot{q}_u \\ &= b\tau + \varphi + S_r, \end{aligned} \tag{2.7}$$

$$\begin{aligned} \text{where } \; b &\triangleq (\Upsilon_a - \Upsilon_u M_{uu}^{-1} M_{au}^T) M_s^{-1}, \\ \varphi &\triangleq (\Upsilon_a - \Upsilon_u M_{uu}^{-1} M_{au}^T) h_a + \Upsilon_u h_u, \\ S_r &\triangleq \Gamma_a \dot{e}_a + \Gamma_u \dot{q}_u. \end{aligned}$$

The control law is designed as

$$\tau = \hat{b}^{-1}(-\Lambda r - S_r - \Delta\tau),\ \Delta\tau = \rho\frac{r}{||r||}, \tag{2.8}$$

where $\Lambda \in \mathbb{R}^{6\times 6}$ is a user-defined positive definite matrix; ρ is the adaptive gain for tackling uncertainties and will be discussed later. Finally, $\hat{b}$ (obtained using the nominal $\hat{M}$) is the nominal value of b which satisfies the condition

$$||b\hat{b}^{-1} - I_6|| \leq E < 1. \tag{2.9}$$

Remark 2 *The value of E can be calculated based on $\hat{M}$ and the upper bound of ΔM (cf. Assumption 2): such condition is quite standard in robotics literature (cf. [59, Ch. 8].*

Substituting (2.8) into (2.7) yields

$$\dot{r} = -\Lambda r - \Delta\tau + \sigma - (b\hat{b}^{-1} - I_6)\Delta\tau, \tag{2.10}$$

where $\sigma \triangleq \varphi - (b\hat{b}^{-1} - I_6)(\Lambda r + S_r)$ represents an uncertainty function. From *Properties 1* and *2*, one can verify

$$||N|| \leq ||C||||\dot{q}|| + ||G|| \leq \bar{c}||\dot{q}||^2 + \bar{g}. \tag{2.11}$$

Let us define $\xi \triangleq [e^T\ \dot{e}^T]^T = [e_a^T\ q_u^T\ \dot{e}_a^T\ \dot{q}_u^T]^T$. Then, using the fact $\dot{e} = \dot{q}$ (as $\dot{q}^d = 0$), Property 1, and the inequalities $||N_u|| \leq ||N||$, $||N_a|| \leq ||N||$, $||d_u|| \leq ||d||$, $||d_a|| \leq ||d||$, $||e_a|| \leq ||\xi||$, $||q_u|| \leq ||\xi||$, $||\dot{e}_a|| \leq ||\xi||$, $||\dot{q}_u|| \leq ||\xi||$ in (2.5), the following bound can be obtained:

$$\begin{aligned} ||\sigma|| &= ||\varphi - (b\hat{b}^{-1} - I_6)(\Lambda r + S_r)|| \\ &\leq ||\varphi|| + E(||\Lambda||||r|| + ||S_r||), \\ &\leq \kappa_0^* + \kappa_1^*||\xi|| + \kappa_2^*||\xi||^2, \\ \text{with } \kappa_0^* &\triangleq a\bar{g} + ||\Upsilon_u||||M_{uu}^{-1}||(\bar{g} + \bar{d}_0) + a_1\bar{d}_0, \\ \kappa_1^* &\triangleq E(||\Gamma_a|| + ||\Gamma_u||) + (||\Upsilon_u||||M_{uu}^{-1}|| + a_1)\bar{d}_1 + a_2, \\ \kappa_2^* &\triangleq a\bar{c} + ||\Upsilon_u||||M_{uu}^{-1}||\bar{c}, \\ a &\triangleq ||(\Upsilon_a - \Upsilon_u M_{uu}^{-1}M_{au})||(||M_s^{-1} + ||M_{au}M_{uu}^{-1}||), \\ a_1 &\triangleq ||(\Upsilon_a - \Upsilon_u M_{uu}^{-1}M_{au})||||M_s^{-1}(1 + ||M_{au}M_{uu}^{-1}||), \\ a_2 &\triangleq E||\Lambda||(||\Upsilon_a|| + ||\Gamma_a|| + ||\Upsilon_u|| + ||\Gamma_u||), \end{aligned} \tag{2.12}$$

where the scalars $\kappa_i^* \in \mathbb{R}^+$, $i = 0, 1, 2$ are *unknown* as per Assumption 2.

Using (2.5a)-(2.5b), the payload swing dynamics can be represented as

$$\begin{aligned}\ddot{q}_u &= -M_{uu}^{-1} M_{au}^T \ddot{q}_a + h_u \\ &= -M_{uu}^{-1} M_{au}^T (M_s^{-1}\tau + h_a) + h_u.\end{aligned} \tag{2.13}$$

Substituting (2.8) into (2.13) yields

$$\begin{aligned}\dot{\chi}_1 &= \chi_2 \\ \dot{\chi}_2 &= -\varpi\upsilon - \varphi_1,\end{aligned} \tag{2.14}$$

where $\chi_1 \triangleq q_u, \chi_2 \triangleq \dot{q}_u, \varphi_1 \triangleq (M_{uu}^{-1} M_{au}^T h_a + h_u), \upsilon \triangleq (-\Lambda r - S_r - \Delta\tau), \varpi \triangleq (M_{uu}^{-1} M_{au}^T M_s^{-1})\hat{b}^{-1}$. A constant full-rank matrix $H \in \mathbb{R}^{2\times 6}$ can be designed such that

$$K_1 \triangleq H\Lambda\Gamma_u,\ K_2 \triangleq H\Lambda\Upsilon_u \tag{2.15}$$

are positive definite matrices. Adding and subtracting $H\upsilon$ to (2.14) yields

$$\begin{aligned}\dot{\chi}_1 &= \chi_2 \\ \dot{\chi}_2 &= -K_1\chi_1 - K_2\chi_2 + \varpi\Delta\tau + \varphi_2,\end{aligned} \tag{2.16}$$

where $\varphi_2 \triangleq \varpi S_r + (H+\varpi)\Lambda r - \varphi_1 - H\Lambda(\Upsilon_a \dot{e}_a + \Gamma_a e_a)$ acts as *uncertainty in the payload swing dynamics*. Taking $\chi \triangleq [\chi_1^T\ \chi_2^T]^T$, $A \triangleq \begin{bmatrix} 0 & I_2 \\ -K_1 & -K_2 \end{bmatrix}$ and $B \triangleq \begin{bmatrix} 0 & I_2 \end{bmatrix}^T$, one has from (2.16)

$$\dot{\chi} = A\chi + B(\varpi\Delta\tau + \varphi_2) \tag{2.17}$$

where positive definiteness of K_1, K_2 guarantees that A is Hurwitz. From *Properties 1-2*, the following holds

$$||\varphi_2||||PB|| \leq \kappa_0^{**} + \kappa_1^{**}||\xi|| + \kappa_2^{**}||\xi||^2, \tag{2.18}$$

$$\begin{aligned}\text{with } \kappa_0^{**} &\triangleq a_3(\bar{d}_0 + \bar{g})||PB||,\ \kappa_2^{**} \triangleq a_3\bar{c}||PB,|| \\ \kappa_1^{**} &\triangleq \{||\varpi||(||\Gamma_a|| + ||\Gamma_u||) + ||H||||\Lambda||(||\Upsilon_a|| + ||\Gamma_a||) \\ &\quad + a_3\bar{d}_1 + a_4\}||PB|| \\ a_3 &\triangleq ||M_{uu}^{-1} M_{au}^T M_s^{-1}||(1 + ||M_{au}^T M_{uu}^{-1}||) + ||M_{uu}^{-1}||||\Upsilon_u|| \\ a_4 &\triangleq (||H|| + ||\varpi||)||\Lambda||(||\Upsilon_a|| + ||\Gamma_a|| + ||\Upsilon_u|| + ||\Gamma_u||)\end{aligned}$$

and $\kappa_i^{**} \in \mathbb{R}^+, i = 0,1,2$ are unknown scalars. $P > 0$ is the solution to the Lyapunov equation $A^T P + PA = -Q$ for some positive definite matrix Q.

Note that the upper bound structures of $||\sigma||$ and $||\varphi_2||$ in (2.12) and (2.18) respectively, are state-dependent in nature via ξ. Accordingly, we design ρ in (2.8) as

$$\rho = \frac{1}{(1-E)}(\hat{\kappa}_0 + \hat{\kappa}_1||\xi|| + \hat{\kappa}_2||\xi||^2 + \gamma), \tag{2.19}$$

with adaptive laws $(i = 0, 1, 2)$

$$\dot{\hat{\kappa}}_i = (||r|| + ||\chi||)||\xi||^i - \hat{\kappa}_i\beta||\chi||||\xi||^i, \tag{2.20a}$$

$$\dot{\gamma} = -\gamma(1 + \gamma_1||\xi||^4) + \nu, \tag{2.20b}$$

$$\beta > 1 + (E_1/(1-E)),\ ||PB\varpi|| \leq E_1, \tag{2.20c}$$

$$\text{with initial conditions } \hat{\kappa}_i(0) > 0,\ \gamma(0) > 0, \tag{2.20d}$$

where $\gamma_1, \nu \in \mathbb{R}^+$ are user-defined scalars and E_1 can be derived from the known upper bound of ΔM in Assumption 2. In (2.20), $\hat{\kappa}_i$ is the estimate of $\max\{\kappa_i^*, \kappa_i^{**}\}$, $i = 0, 1, 2$, while γ helps in swing angle and closed-loop system stabilization.

The proposed control framework is depicted via a block-diagram in Fig. 2.2 and, further, is summarized via Algorithm 1.

Algorithm 1: Design steps of the proposed controller

---

1. **Step 0 (Designing (offline) gain parameters):** Define gains $\Upsilon_a, \Gamma_a, \Upsilon_u, \Gamma_u, \Lambda$ and select $\hat{b}$ from (2.9).
2. **Step 1 (Defining the error variables):** Find error e_a and compute auxiliary error variable r with gains defined in Step 0 as in (2.6).
3. **Step 2 (Designing adaptive gains):** Compute the gain ρ from (2.19) using the adaptive laws in (2.20).
4. **Step 3 (Computing τ and U):** Compute control input τ from (2.8) and then, U from τ_p as per (2.1b).
5. **Step 4 (Control input to system):** Finally, apply U and τ_q to the quadrotor.

The closed-loop stability result is presented subsequently.

Theorem 1 *Under Properties 1-2 and Assumptions 1-2, the closed-loop trajectories of (2.5) employing the proposed controller (2.8), (2.19) with gain conditions (2.9), (2.15) and adaptive laws (2.20) are Uniformly Ultimately Bounded (UUB).*

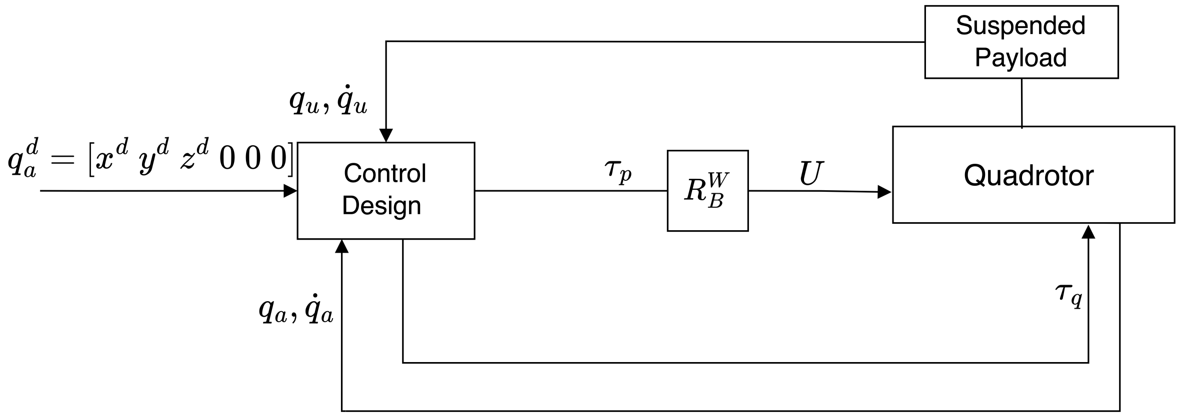

Figure 2.2: Proposed control framework

Remark 3 (Continuous control law) *To make the control law continuous and avoid chattering in practice, $\Delta\tau$ in (2.8) can be modified via smooth sigmoid functions as $\Delta\tau = \rho\frac{r}{\sqrt{||r||^2+\epsilon}}$ with ϵ being a positive scalar. Such modifications only lead to minor modifications in stability analysis without changing the stability results (cf. [61]), and hence, repetition is avoided.*

2.4 Stability Analysis

From the adaptive law (2.20b) and initial condition (2.20d), it can be verified that $\exists\underline{\gamma}, \overline{\gamma} \in \mathbb{R}^+$ such that

$$0 < \underline{\gamma} \leq \gamma(t) \leq \overline{\gamma} \ \ \forall t \geq 0. \tag{2.21}$$

Stability is analyzed via the Lyapunov function:

$$V = \frac{1}{2}r^T r + \frac{1}{2}\chi^T P\chi + \frac{1}{2}\sum_{i=0}^{2}(\hat{\kappa}_i - \bar{\kappa}_i^*)^2 + \frac{\gamma}{\underline{\gamma}}, \tag{2.22}$$

where $\bar{\kappa}_i^* = \max\{\kappa_i^*, \kappa_i^{**}\}$.

Using (2.8), (2.12) and (2.19), from (2.7) we have

$$\begin{aligned} r^T\dot{r} &= r^T(-\Lambda r - \Delta\tau + \sigma - (b\hat{b}^{-1} - I_6)\Delta\tau) \\ &\leq -r^T\Lambda r - (1-E)\rho||r|| + \sum_{i=0}^{2}\kappa_i^*||\xi||^i||r|| \\ &\leq -r^T\Lambda r - \sum_{i=0}^{2}\hat{\kappa}_i||\xi||^i||r|| + \bar{\kappa}_i^*||\xi||^i||r||. \end{aligned} \tag{2.23}$$

where we have used the fact that $\gamma > 0$ from (2.21). Further, using (2.17) and (2.18) we have

$$\begin{aligned}\frac{1}{2}\frac{\mathrm{d}}{\mathrm{d}t}\chi^T P\chi &= -\frac{1}{2}\chi^T Q\chi + \chi^T PB(\varpi\Delta\tau + \varphi_2)\\ &\le -\frac{1}{2}\chi^T Q\chi + \rho E_1||\chi|| + ||\varphi_2||||PB||||\chi||\\ &\le -\frac{1}{2}\chi^T Q\chi + \sum_{i=0}^{2}(\bar{\kappa}_i^*||\xi||^i + \frac{E_1(\hat{\kappa}_i||\xi||^i + \gamma)}{1-E})||\chi||. \end{aligned}\tag{2.24}$$

Using the adaptive laws (2.20a), (2.20b), and (2.21) we have

$$\begin{aligned}(\hat{\kappa}_i - \bar{\kappa}_i^*)\dot{\hat{\kappa}}_i &= \hat{\kappa}_i(||r|| + ||\chi||)||\xi||^i - \beta\hat{\kappa}_i^2||\chi||||\xi||^i\\ &\quad - \bar{\kappa}_i^*(||r|| + ||\chi||)||\xi||^i + \beta\hat{\kappa}_i\bar{\kappa}_i^*||\chi||||\xi||^i, \end{aligned}\tag{2.25}$$

$$\frac{\dot{\gamma}}{\underline{\gamma}} = -\frac{\gamma}{\underline{\gamma}}(1 + \gamma_1||\xi||^4) + \frac{\nu}{\underline{\gamma}} \le -\gamma_1||\xi||^4 + (\nu/\underline{\gamma}),\tag{2.26}$$

where we have used the fact that $\gamma \ge \underline{\gamma}$ from (2.21). Using (2.23)-(2.26), the time derivative of the Lyapunov function (2.22) turns out to satisfy

$$\begin{aligned}\dot{V} \le &- \delta_m(||r||^2 + ||\chi||^2) - \gamma_1||\xi||^4 + (\nu/\underline{\gamma}) + c\gamma||\chi||\\ &+ \sum_{i=0}^{2}(c\hat{\kappa}_i - \beta\hat{\kappa}_i^2 + \beta\hat{\kappa}_i\bar{\kappa}_i^*)||\xi||^i||\chi||, \end{aligned}\tag{2.27}$$

where $\delta_m \triangleq \min\{\lambda_{\min}(\Lambda),\ (1/2)\lambda_{\min}(Q)\}$ and $c \triangleq 1 + \frac{E_1}{1-E}$. From (2.22), the definition of V yields

$$V \le \delta_M(||r||^2 + ||\chi||^2) + \sum_{i=0}^{2}(\hat{\kappa}_i^2 + {\bar{\kappa}_i^*}^2) + \frac{\bar{\gamma}}{\underline{\gamma}},\tag{2.28}$$

where $\delta_M \triangleq \max\{1,\ ||P||\}$. Defining $\Omega \triangleq (\delta_m/\delta_M)$, (2.27) is further simplified using (2.28) as

$$\begin{aligned}\dot{V} &\le -\Omega V - \gamma_1||\xi||^4 + (\nu/\underline{\gamma}) + (\Omega\bar{\gamma})/\underline{\gamma} + c\gamma||\chi||\\ &+ \sum_{i=0}^{2}(c\hat{\kappa}_i - \beta\hat{\kappa}_i^2 + \beta\hat{\kappa}_i\bar{\kappa}_i^*)||\xi||^i||\chi|| + \Omega(\hat{\kappa}_i^2 + \bar{\kappa}_i^*)^2. \end{aligned}\tag{2.29}$$

Since $\beta > 1$ by design (2.20c), it is always possible to split β as $\beta = \beta_1 + \beta_2 + \beta_3$ where $\beta_i > 0$, $i = 1, 2, 3$. Then, the following simplification can be made

$$\begin{aligned}
-\beta\hat{\kappa}_i^2 + c\hat{\kappa}_i + \beta\hat{\kappa}_i\bar{\kappa}_i^* &= -\beta_1\hat{\kappa}_i^2 - \beta_2\left\{\left(\hat{\kappa}_i - \frac{c}{2\beta_2}\right)^2 - \frac{c^2}{4\beta_2^2}\right\} \\
&\quad - \beta_3\left\{\left(\hat{\kappa}_i - \frac{\beta\bar{\kappa_i^*}}{2\beta_3}\right)^2 - \frac{(\beta\bar{\kappa_i^*})^2}{4\beta_3^2}\right\} \\
&\leq -\beta_1\hat{\kappa}_i^2 + \frac{c^2}{4\beta_2} + \frac{(\beta\bar{\kappa}_i^*)^2}{4\beta_3}.
\end{aligned} \tag{2.30}$$

Using (2.30), the inequality (2.29) becomes

$$\dot{V} \leq -\Omega V - \sum_{i=0}^{2}(\beta_1||\chi||^{(i+1)} - \Omega)\hat{\kappa}_i^2 + f(||\xi||), \tag{2.31}$$

$$\begin{aligned}
&\text{where } f(||\xi||) \triangleq -\gamma_1||\xi||^4 + \varsigma_3||\xi||^3 + \varsigma_2||\xi||^2 + \varsigma_1||\xi|| + \varsigma_0, \\
&\quad \varsigma_3 \triangleq c^2/(4\beta_2) + (\beta\bar{\kappa}_2^*)^2/(4\beta_3), \\
&\quad \varsigma_2 \triangleq \frac{c^2}{4\beta_2} + \frac{(\beta\bar{\kappa}_1^*)^2}{4\beta_3}, \varsigma_1 \triangleq \frac{c^2}{2\beta_2} + \frac{(\beta\bar{\kappa}_0^*)^2}{4\beta_3} + c\bar{\gamma}, \\
&\quad \varsigma_0 \triangleq \Omega(\bar{\kappa}_0^{*2} + \bar{\kappa}_1^{*2} + \bar{\kappa}_2^{*2}) + (\nu/\underline{\gamma}) + (\Omega\bar{\gamma})/\underline{\gamma}.
\end{aligned}$$

Bolzano's Theorem and Descartes' rule of sign change imply that the polynomial f has finite positive real roots; let $\iota \in \mathbb{R}^+$ be the maximum positive real root of f. Since the coefficient of the highest degree of f is negative as $\gamma_1 \in \mathbb{R}^+$, $f(||\xi||) \leq 0$ when $||\xi|| \geq \iota$. This was possible owing to the negative fourth degree term $-\gamma_1||\xi||^4$ contributed by $\dot{\gamma}$. Define $\iota_1 \triangleq \max\{(\Omega/\beta_1), (\Omega/\beta_1)^{\frac{1}{2}}, (\Omega/\beta_1)^{\frac{1}{3}}\}$. Hence, from (2.31), $\dot{V} \leq -\Omega V$ when

$$\begin{aligned}
\min\{||\chi||, ||\xi||\} &\geq \max\{\iota,\ \iota_1\} \\
&\Rightarrow ||\chi|| \geq \max\{\iota,\ \iota_1\},
\end{aligned} \tag{2.32}$$

implying that the closed-loop system is UUB and $r, q_u, \dot{q}_u, \hat{\kappa}_i, \gamma$ remain bounded; again, boundedness of $r, q_u, \dot{q}_u$ ensures that $e_a, \dot{e}_a$ are bounded from (2.6).

Chapter 3

Experimental Results

3.0.1 The Experimental Setup

The proposed controller is tested on a quadrotor setup (Q-450 frame with Turnigy SK3-2826 brushless motors, weighing ~ 1.5 kg), with a payload (~ 0.2 kg) suspended from its center. Raspberry Pi-4 is used as a processing unit and joystick potentiometer is used to measure swing angles of payload (cf. [58] for such arrangement). Optitrack motion capture system (at 120 fps) and IMU were used to obtain system pose and state-derivatives were obtained via fusing these sensor data for the necessary feedback.

To verify the effectiveness of the proposed control law, we compare it with the adaptive method [50].

3.0.2 Parameter Selection

The following control design parameters are selected for the proposed controller during the experimentation: $\Upsilon_a = diag\{1, 1, 3, 2, 2, 2\},\ \Gamma_a = diag\{1, 1, 2, 4, 4, 4\}$,
$\Upsilon_u = \begin{bmatrix} 0.02 & 0 & 0 & 0 & 0 & 0 \\ 0 & 0.02 & 0 & 0 & 0 & 0 \end{bmatrix}^T, \Gamma_u = 2.5\Upsilon_u, \hat{b} = diag\{1.5, 1.5, 1.5, 0.02, 0.02, 0.04\},\ E = 0.3$,
$\hat{\kappa}_0(0) = \hat{\kappa}_1(0) = \hat{\kappa}_2(0) = 0.01, \gamma(0) = 0.1,\ \Lambda = diag\{1.0, 1.0, 1.2, 0.5, 0.5, 0.2\},\ \eta_0 = 2, \eta_1 = 3, \eta_2 = 1,\ \zeta_0 = 1, \zeta_1 = 2, \zeta_2 = 1,\ \beta = 3,\ \gamma_0 = 2, \gamma_1 = 1, \gamma_2 = 2,\ \nu = 0.001,\ \epsilon = 0.1$.
For the adaptive controller [50], the various control parameters are selected as in [50].

3.0.3 Experimental Scenario

During payload delivery operation via cable-suspended mode, human interacts closely with the quadrotor while attaching or detaching the payload; during such interaction, payload swing can happen and if not properly stabilized, such swings can cause safety hazard. We have created an experimental scenario in an attempt to emulate such phenomenon (cf. Fig. 1.5): in this scenario, the quadrotor hovers at a given position ($x^d = y^d = 0, z^d = 1$m) and, suddenly, the payload is pushed by a stick at $t = 2$s (approx.) to create swing angles. As mentioned before in Remark 2, the motion in swing angles create state-dependent uncertainty. Therefore, such an experimental scenario tests the capability of a controller to negotiate state-dependent disturbances. Additionally, a fan is used to introduce wind disturbance.

3.0.4 Results and Discussion

The performances of the controllers are compared via Figs. 3.1-3.3 and via Table 3.1. The red marked zones in Figs. 3.3-3.3 highlight the oscillations caused by the stick.

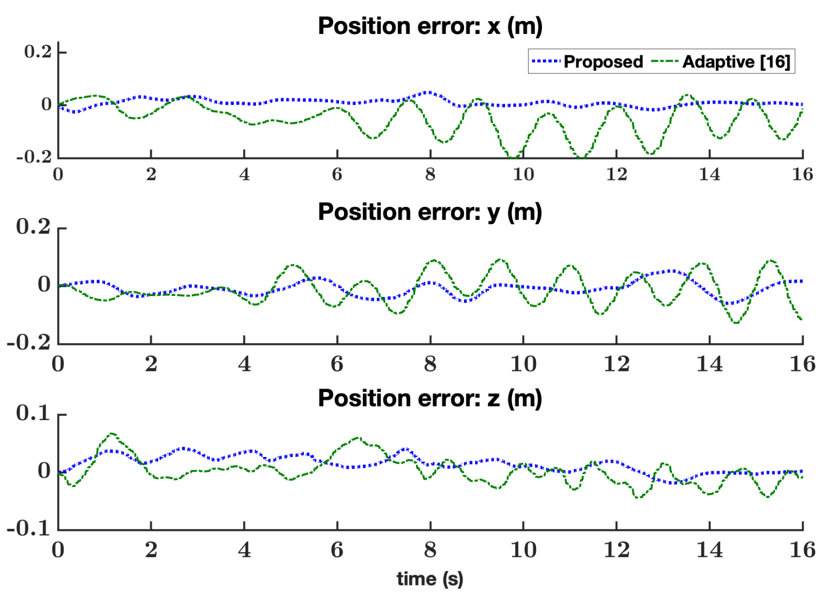

Figure 3.1: Quadrotor position tracking error.

It can be observed that the proposed controller could successfully damp the swing angle oscillations even with higher initial overshoots compared to the other controllers. Whereas, in absence of any measure to deal with state-dependent uncertainty, [50] fails to damp the oscillations in swing angles leading to sustained oscillations and drift in the quadrotor positions

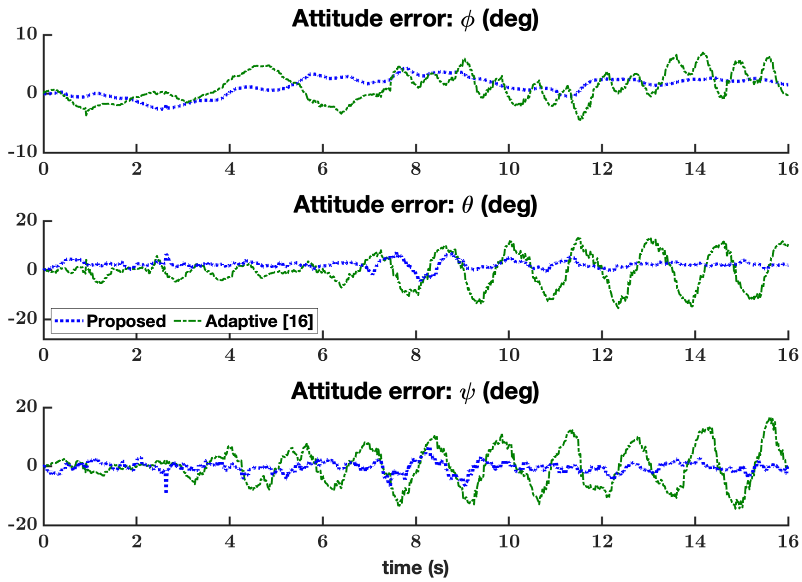

Figure 3.2: Quadrotor attitude tracking error.

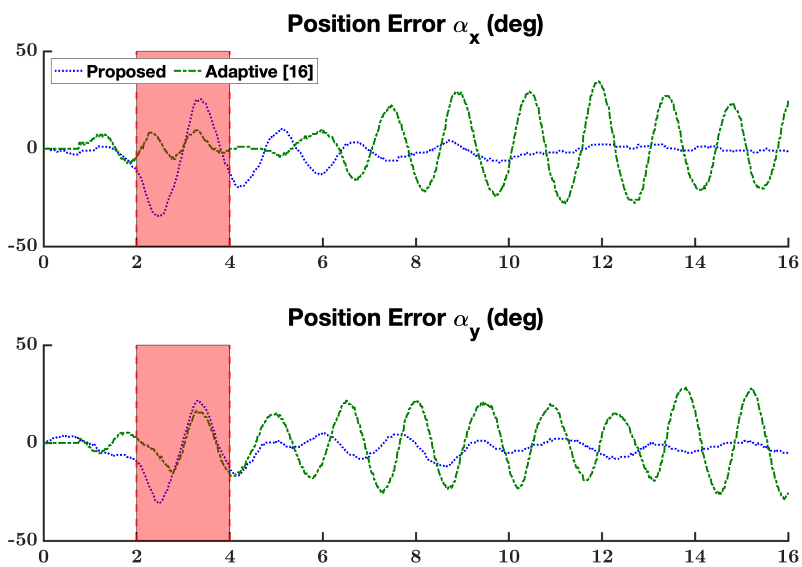

Figure 3.3: Stabilization error in payload swing angles α_x and α_y.

(cf. Fig. 3.1 after $t = 2$s). This can cause hazard to human operator. Interestingly, the proposed scheme without γ is significantly slow in damping the oscillations and suffers from drifting in quadrotor. This demonstrates the importance of γ in overall control performance and system stabilization.

Table 3.1: Root-Mean-Squared (RMS) error comparison

Controller	Position error (m)			Attitude error (deg)		
	x	y	z	ϕ	θ	ψ
Proposed	**0.02**	**0.06**	**0.02**	**3.5**	**3.1**	**3.8**
Adaptive [50]	0.08	0.08	0.12	14.8	13.05	6.6
Controller			Swing angle error (deg)			
			α_x	α_y		
Proposed			**8.5**	**6.9**		
Adaptive [50]			15.1	15.9		

The data presented in Table 3.1 showcases a comparative analysis of Root-Mean-Squared (RMS) error performance between the proposed controller and an existing adaptive controller from the literature [50]. The proposed controller demonstrates superior performance across all measured parameters. Specifically, in terms of position error (measured in meters), the proposed controller achieves the lowest errors with 0.02 in the x and z axes, and 0.06 in the y axis. In contrast, the adaptive controller records higher errors of 0.08 in both the x and y axes and 0.12 in the z axis. Similarly, for attitude error (measured in degrees), the proposed controller maintains lower errors (3.5, 3.1, and 3.8 degrees in ϕ, θ, and ψ respectively) compared to the adaptive controller (14.8, 13.05, and 6.6 degrees). Moreover, the proposed controller also exhibits better control in minimizing swing angle errors, with 8.5 degrees in α_x and 6.9 degrees in α_y, significantly lower than the 15.1 and 15.9 degrees recorded by the adaptive controller. These results clearly indicate the enhanced accuracy and efficiency of the proposed controller in managing both position and orientation aspects of quadrotor control, as well as in reducing swing angles, which is crucial for operational stability and precision.

Chapter 4

Conclusion and Future Work

4.1 Conclusion

In this thesis, an adaptive control was proposed for safe human interaction for quadrotors with suspended payloads.

In summary, this research has introduced and evaluated an effective adaptive anti-swing controller tailored for human-quadrotor interaction during the clasping and unclasping of cable-suspended payloads. The appropriateness of this solution stems from its unique ability, unlike existing approaches, to manage unknown state-dependent uncertainties inherent in these dynamics. Notably, the designed controller is adept at addressing such uncertainties without requiring a priori knowledge of their specific terms. Experimental investigations demonstrated the safety and superior performance of the proposed control framework. In comparison to state-of-the-art methods, the adaptive solution showcased a remarkable capacity to mitigate undesired payload swings, signifying its efficacy and potential for enhancing the safety and precision of human-quadrotor interactions in such scenarios.

4.2 Future Works

- In forthcoming research, it becomes essential to shift from the current emphasis on hovering control to embrace a more comprehensive six degrees-of-freedom framework for dynamic payload lifting operations. The development of a future controller should capitalize on the partially decoupled dynamics, employing a switched mode control strategy to effectively manage the complexities associated with multidimensional motion.

- The adaptive controllers devised in this thesis do not address scenarios involving maneuvering within specific motion constraints. Consequently, an intriguing avenue for future research would involve extending the proposed adaptive designs to account for both position and velocity constraints in the context of quadrotors with suspended payloads.
- Throughout the thesis, the external payloads are considered to be suspended from the center of mass of the quadrotor platform. The case of payload transportation via a manipulator could considered in future which brings its own coupling challenges that could be tackled adaptively.

Related Publications

1. **Adaptive Anti-swing Control for Clasping Operations in Quadrotors with Cable-suspended Payload**
   Ananth Rachakonda*, Swati Dantu*, Rishabh Dev Yadav*, Spandan Roy, and Simone Baldi, *62nd IEEE Conference on Decision and Control (CDC)*, Singapore, 2023.

   * joint first author.

Bibliography

[1] Taeyoung Lee, Melvin Leok, and N Harris McClamroch. Geometric tracking control of a quadrotor uav on se (3). In *49th IEEE Conference on Decision and Control (CDC)*, pages 5420–5425. IEEE, 2010.

[2] Fadri Furrer, Michael Burri, Markus Achtelik, and Roland Siegwart. *RotorS – A Modular Gazebo MAV Simulator Framework*, volume 625, pages 595–625. 01 2016.

[3] Kumar V. Mellinger D., Michael N. Trajectory generation and control for precise aggressive maneuvers with quadrotors. In *Experimental Robotics. Springer Tracts in Advanced Robotics, vol 79*. Springer, Berlin, Heidelberg., 2014.

[4] S. Bouabdallah, P. Murrieri, and R. Siegwart. Design and control of an indoor micro quadrotor. In *IEEE International Conference on Robotics and Automation, 2004. Proceedings. ICRA '04. 2004*, volume 5, pages 4393–4398 Vol.5, 2004.

[5] S. Bouabdallah, A. Noth, and R. Siegwart. Pid vs lq control techniques applied to an indoor micro quadrotor. In *2004 IEEE/RSJ International Conference on Intelligent Robots and Systems (IROS) (IEEE Cat. No.04CH37566)*, volume 3, pages 2451–2456 vol.3, 2004.

[6] S. Bouabdallah, P. Murrieri, and R. Siegwart. Towards autonomous indoor micro vtol. In *Auton Robot*, volume 18, pages 171–183, 2005.

[7] Wenwu Yu, ZeFang He, and Long Zhao. A simple attitude control of quadrotor helicopter based on ziegler-nichols rules for tuning pd parameters. *The Scientific World Journal*, 2014.

[8] Long Chen and Gang Wang. Attitude stabilization for a quadrotor helicopter using a pd controller. *International Conference on Intelligent Control and Automation Science*, 2013.

[9] S. Nadda and A. Swarup. Decoupled control design for robust performance of quadrotor. *Int. J. Dynam. Control 6*, page 1367–1375, 2018.

[10] H. & Sastry S. Lee, D. & Jin Kim. Feedback linearization vs. adaptive sliding mode control for a quadrotor helicopter. *Int. J. Control Autom. Syst.*, 7:419–428, 2009.

[11] Daniel Mellinger and Vijay Kumar. Minimum snap trajectory generation and control for quadrotors. In *2011 IEEE International Conference on Robotics and Automation*, pages 2520–2525. IEEE, 2011.

[12] Dawei Shen, Qiang Lu, Min Hu, and Zhiwei Kong. Mathematical modeling and control of the quad tilt-rotor uav. In *2018 IEEE 8th Annual International Conference on CYBER Technology in Automation, Control, and Intelligent Systems (CYBER)*, pages 1220–1225, 2018.

[13] Siddharth Sridhar, Gaurang Gupta, Rumit Kumar, Manish Kumar, and Kelly Cohen. Tilt-rotor quadcopter xplored: Hardware based dynamics, smart sliding mode controller, attitude hold wind disturbance scenarios. In *2019 American Control Conference (ACC)*, pages 2005–2010, 2019.

[14] Jinho Kim, S. Andrew Gadsden, and Stephen A. Wilkerson. A comprehensive survey of control strategies for autonomous quadrotors. *Canadian Journal of Electrical and Computer Engineering*, 43(1):3–16, 2020.

[15] J Thomas, J Polin, K Sreenath, and V. Kumar. Avian-inspired grasping for quadrotor micro uavs. *ASME 2013 International Design Engineering Technical Conferences and Computers and Information in Engineering Conference. Volume 6A: 37th Mechanisms and Robotics Conference. Portland, Oregon, USA. August 4–7, 2013*, 6A, 2013.

[16] Sarah Tang and Vijay Kumar. Mixed integer quadratic program trajectory generation for a quadrotor with a cable-suspended payload. In *2015 IEEE International Conference on Robotics and Automation (ICRA)*, pages 2216–2222. IEEE, 2015.

[17] Sen Yang and Bin Xian. Energy-based nonlinear adaptive control design for the quadrotor uav system with a suspended payload. *IEEE Transactions on Industrial Electronics*, 2019.

[18] Pedro Pereira, Jorge Cortés, and Dimos V Dimarogonas. Aerial slung-load position tracking under unknown wind forces. *IEEE Trans. Autom. Control*, 66(9):3952–3968, 2020.

[19] Davide Invernizzi, Marco Lovera, and Luca Zaccarian. Integral iss-based cascade stabilization for vectored-thrust uavs. *IEEE Control Systems Letters*, 4(1):43–48, 2019.

[20] Lorenzo Fusini, Thor I Fossen, and Tor Arne Johansen. Nonlinear observers for gnss- and camera-aided inertial navigation of a fixed-wing uav. *IEEE Transactions on Control Systems Technology*, 26(5):1884–1891, 2018.

[21] Koushil Sreenath, Nathan Michael, and Vijay Kumar. Trajectory generation and control of a quadrotor with a cable-suspended load - a differentially-flat hybrid system. In *2013 IEEE Int. Conf. Robot. Autom.*, pages 4888–4895, 2013.

[22] Sen Yang and Bin Xian. Energy-based nonlinear adaptive control design for the quadrotor uav system with a suspended payload. *IEEE Trans. Ind. Electron.*, 67(3):2054–2064, 2020.

[23] Bin Xian and Sen Yang. Robust tracking control of a quadrotor unmanned aerial vehicle-suspended payload system. *IEEE/ASME Trans. Mechatron.*, 26(5):2653–2663, 2021.

[24] Viswa N. Sankaranarayanan, Spandan Roy, and Simone Baldi. Aerial transportation of unknown payloads: Adaptive path tracking for quadrotors. In *IEEE/RSJ Int. Conf. Intell. Robots Syst. (IROS)*, pages 7710–7715, 2020.

[25] Brendan J Bialy, Justin Klotz, K Brink, and Warren E Dixon. Lyapunov-based robust adaptive control of a quadrotor uav in the presence of modeling uncertainties. In *2013 American Control Conference*, pages 13–18. IEEE, 2013.

[26] Giuseppe Loianno, Vojtech Spurny, Justin Thomas, Tomas Baca, Dinesh Thakur, Daniel Hert, Robert Penicka, Tomas Krajnik, Alex Zhou, Adam Cho, et al. Localization, grasping, and transportation of magnetic objects by a team of mavs in challenging desert-like environments. *IEEE Rob. Autom. Lett.*, 3(3):1576–1583, 2018.

[27] Bo Zhao, Bin Xian, Yao Zhang, and Xu Zhang. Nonlinear robust sliding mode control of a quadrotor unmanned aerial vehicle based on immersion and invariance method. *International Journal of Robust and Nonlinear Control*, 25(18):3714–3731, 2015.

[28] Sergey G Nersesov, Hashem Ashrafiuon, and Parham Ghorbanian. On estimation of the domain of attraction for sliding mode control of underactuated nonlinear systems. *International Journal of Robust and Nonlinear Control*, 24(5):811–824, 2014.

[29] Velupillai Sankaranarayanan and Arun D Mahindrakar. Control of a class of underactuated mechanical systems using sliding modes. *IEEE Transactions on Robotics*, 25(2):459–467, 2009.

[30] Rong Xu and Ümit Özgüner. Sliding mode control of a class of underactuated systems. *Automatica*, 44(1):233–241, 2008.

[31] Shafiqul Islam, Peter X Liu, and Abdulmotaleb El Saddik. Robust control of four-rotor unmanned aerial vehicle with disturbance uncertainty. *IEEE Trans. Ind. Electron.*, 62(3):1563–1571, 2015.

[32] C Nicol, CJB Macnab, and A Ramirez-Serrano. Robust adaptive control of a quadrotor helicopter. *Mechatronics*, 21(6):927–938, 2011.

[33] Zachary T Dydek, Anuradha M Annaswamy, and Eugene Lavretsky. Adaptive control of quadrotor uavs: A design trade study with flight evaluations. *IEEE Transactions on control systems technology*, 21(4):1400–1406, 2012.

[34] ChangSu Ha, Zhiyuan Zuo, Francis B Choi, and Dongjun Lee. Passivity-based adaptive backstepping control of quadrotor-type uavs. *Robotics and Autonomous Systems*, 62(9):1305–1315, 2014.

[35] Trong-Toan Tran, Shuzhi Sam Ge, and Wei He. Adaptive control of a quadrotor aerial vehicle with input constraints and uncertain parameters. *International Journal of Control*, 91(5):1140–1160, 2018.

[36] Bailing Tian, Jie Cui, Hanchen Lu, Zongyu Zuo, and Qun Zong. Adaptive finite-time attitude tracking of quadrotors with experiments and comparisons. *IEEE Transactions on Industrial Electronics*, 2019.

[37] Bo Zhao, Bin Xian, Yao Zhang, and Xu Zhang. Nonlinear robust adaptive tracking control of a quadrotor uav via immersion and invariance methodology. *IEEE Transactions on Industrial Electronics*, 62(5):2891–2902, 2014.

[38] Spandan Roy, Simone Baldi, and Leonid M Fridman. On adaptive sliding mode control without a priori bounded uncertainty. *Automatica*, page 108650, 2019.

[39] Spandan Roy and Indra Narayan Kar. Adaptive-robust control for systems with state-dependent upper bound in uncertainty. In *Adaptive-Robust Control with Limited Knowledge on Systems Dynamics*, pages 117–142. Springer, 2020.

[40] Guanyu Lai, Zhi Liu, Yun Zhang, CL Philip Chen, and Shengli Xie. Adaptive backstepping-based tracking control of a class of uncertain switched nonlinear systems. *Automatica*, 91:301–310, 2018.

[41] Shuai Yuan, Bart De Schutter, and Simone Baldi. Robust adaptive tracking control of uncertain slowly switched linear systems. *Nonlinear Analysis: Hybrid Systems*, 27:1–12, 2018.

[42] Shuai Yuan, Fan Zhang, and Simone Baldi. Adaptive tracking of switched nonlinear systems with prescribed performance using a reference-dependent reparametrisation approach. *International Journal of Control*, 92(6):1243–1251, 2019.

[43] Zhi-E Lou and Jun Zhao. Immersion-and invariance-based adaptive stabilization of switched nonlinear systems. *International Journal of Robust and Nonlinear Control*, 28(1):197–212, 2018.

[44] Weisheng Chen, Changyun Wen, and Jian Wu. Global exponential/finite-time stability of nonlinear adaptive switching systems with applications in controlling systems with unknown control direction. *IEEE Transactions on Automatic Control*, 2018.

[45] Jun Ye, Spandan Roy, Milinko Godjevac, Vasso Reppa, and Simone Baldi. Robustifying dynamic positioning of crane vessels for heavy lifting operation. *IEEE/CAA Journal of Automatica Sinica*, 8(4):753–765, 2021.

[46] Longhao Qian and Hugh HT Liu. Path-following control of a quadrotor uav with a cable-suspended payload under wind disturbances. *IEEE Trans. Ind. Electron.*, 67(3):2021–2029, 2019.

[47] David Cabecinhas, Rita Cunha, and Carlos Silvestre. A trajectory tracking control law for a quadrotor with slung load. *Automatica*, 106:384–389, 2019.

[48] Hean Hua, Yongchun Fang, Xuetao Zhang, and Chen Qian. A new nonlinear control strategy embedded with reinforcement learning for a multirotor transporting a suspended payload. *IEEE/ASME Trans. Mechatron.*, 27(2):1174–1184, 2022.

[49] Gan Yu, Wei Xie, David Cabecinhas, Rita Cunha, and Carlos Silvestre. Adaptive control with unknown mass estimation for a quadrotor-slung-load system. *ISA Trans.*, 133:412–423, 2023.

[50] Xiao Liang, Yongchun Fang, Ning Sun, He Lin, and Xingang Zhao. Adaptive nonlinear hierarchical control for a rotorcraft transporting a cable-suspended payload. *IEEE Trans. Syst. Man Cybern.: Syst.*, 51(7):4171–4182, 2021.

[51] Zong-Yang Lv, Shengming Li, Yuhu Wu, and Qing-Guo Wang. Adaptive control for a quadrotor transporting a cable-suspended payload with unknown mass in the presence of rotor downwash. *IEEE Trans. Veh. Technol.*, 70(9):8505–8518, 2021.

[52] Xiao Liang, Yongchun Fang, Ning Sun, and He Lin. A novel energy-coupling-based hierarchical control approach for unmanned quadrotor transportation systems. *IEEE/ASME Trans. Mechatron.*, 24(1):248–259, 2019.

[53] Swati Dantu, Rishabh Dev Yadav, Spandan Roy, Jinoh Lee, and Simone Baldi. Adaptive artificial time delay control for quadrotors under state-dependent unknown dynamics. In *2022 IEEE Int. Conf. Robot. Biomim.*, pages 1092–1097. IEEE, 2022.

[54] Viswa N Sankaranarayanan, Rishabh D Yadav, Rahul K Swayampakula, Sourish Ganguly, and Spandan Roy. Robustifying payload carrying operations for quadrotors under time-varying state constraints and uncertainty. *IEEE Rob. Autom. Lett.*, 7(2):4885–4892, 2022.

[55] Spandan Roy, Simone Baldi, Peng Li, and Viswa Narayanan. Artificial-delay adaptive control for under-actuated euler-lagrange robotics. *IEEE/ASME Transactions on Mechatronics*, 2021.

[56] Xiao Liang, Yongchun Fang, Ning Sun, He Lin, and Xingang Zhao. Adaptive nonlinear hierarchical control for a rotorcraft transporting a cable-suspended payload. *IEEE Trans. Syst. Man Cybern.: Syst.*, 51(7):4171–4182, 2019.

[57] Maria Eusebia Guerrero, DA Mercado, Rogelio Lozano, and CD García. Passivity based control for a quadrotor uav transporting a cable-suspended payload with minimum swing. In *2015 54th IEEE Conf. Decis. Control*, pages 6718–6723. IEEE, 2015.

[58] M Eusebia Guerrero-Sánchez, D Alberto Mercado-Ravell, Rogelio Lozano, and C Daniel García-Beltrán. Swing-attenuation for a quadrotor transporting a cable-suspended payload. *ISA Trans.*, 68:433–449, 2017.

[59] Mark W Spong, Seth Hutchinson, and Mathukumalli Vidyasagar. *Robot modeling and control*. Wiley New York, 2006.

[60] Randal W Beard and Timothy W McLain. *Small unmanned aircraft: Theory and practice*. Princeton University Press, 2012.

[61] Spandan Roy, Jinoh Lee, and Simone Baldi. A new adaptive-robust design for time delay control under state-dependent stability condition. *IEEE Trans. Control Syst. Technol.*, 29(1):420–427, 2020.